
Figures and figure supplements

The RNA helicase DDX39B activates FOXP3 RNA splicing to control T regulatory cell fate

Minato Hirano and Gaddiel Galarza-Muñoz *et al.*

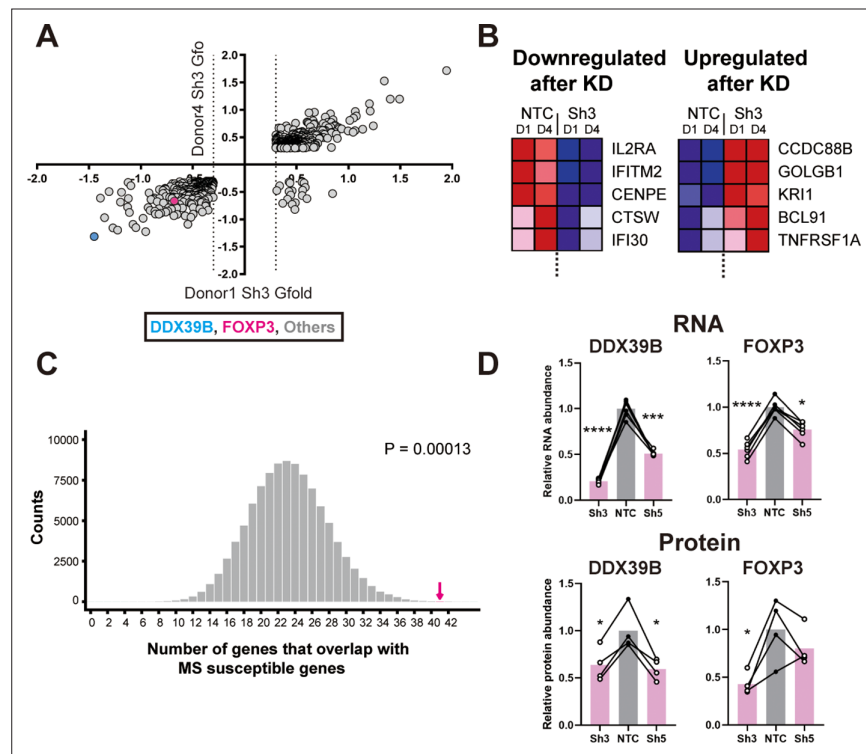


Figure 1. Loss of FOXP3 expression in DDX39B-depleted T cells. **(A)** RNA abundance changes between control (NTC) and DDX39B-depleted (Sh3) CD4⁺ T cells from two healthy individuals (Donor 1 and Donor 4) identified by RNAseq. Data points for DDX39B (cyan) and FOXP3 (magenta) are indicated. **(B)** Examples of MS susceptibility genes differentially expressed upon DDX39B knockdown. The heat map shows expression of five genes between control (NTC) and DDX39B depleted (Sh3) CD4⁺ T cells. **(C)** Enrichment analysis of MS susceptibility genes in DEGs following DDX39B depletion. Resampling 100,000 times resulted in a distribution of the number of genes that overlap by chance, with 23 being the most common result. The observed overlap of 41 (Magenta arrow) demonstrates substantial enrichment (empirical $p=0.00013$). **(D)** Levels of DDX39B RNA and FOXP3 RNA, normalized to *EEF1A1* RNA levels, after DDX39B depletion in CD4⁺ T cells and levels of DDX39B and FOXP3 protein relative to Tubulin after DDX39B depletion in CD4⁺ T cells. Connected dots indicate samples from the same donor. In all figures the error bars indicate standard deviation. *: $p<0.05$, **: $p<0.01$, ***: $p<0.001$ and ****: $p<0.0001$.

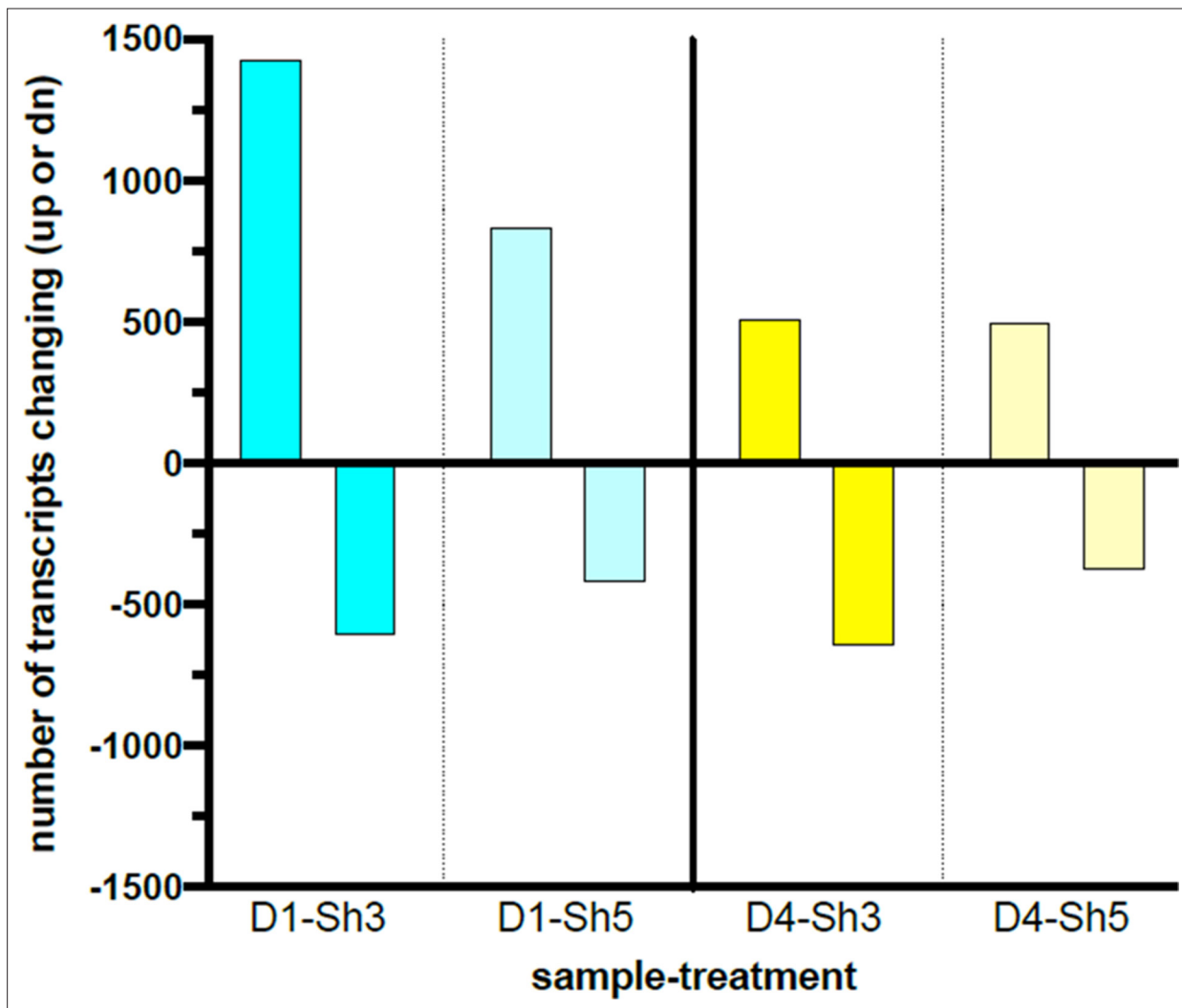


Figure 1—figure supplement 1. Transcript level changes upon DDX39B depletion in primary human CD4⁺ T cells. DDX39B was depleted in primary CD4⁺ T cells from two healthy donors (donors 1 and 4) using DDX39B targeting (Sh3 and Sh5) shRNAs. RNAseq was used to examine transcript level changes between these cells and those treated with control (NTC) shRNA. The figure illustrates the comparison of the transcripts whose expression changed significantly (up or down) for each donor and shRNA combination. Criteria for inclusion were (a) transcripts were required to have RPKM ≥ 2 and (b) transcript level changes between conditions had $|\text{Gfold values}| \geq 0.3$ for Sh3 or ≥ 0.1 for Sh5.

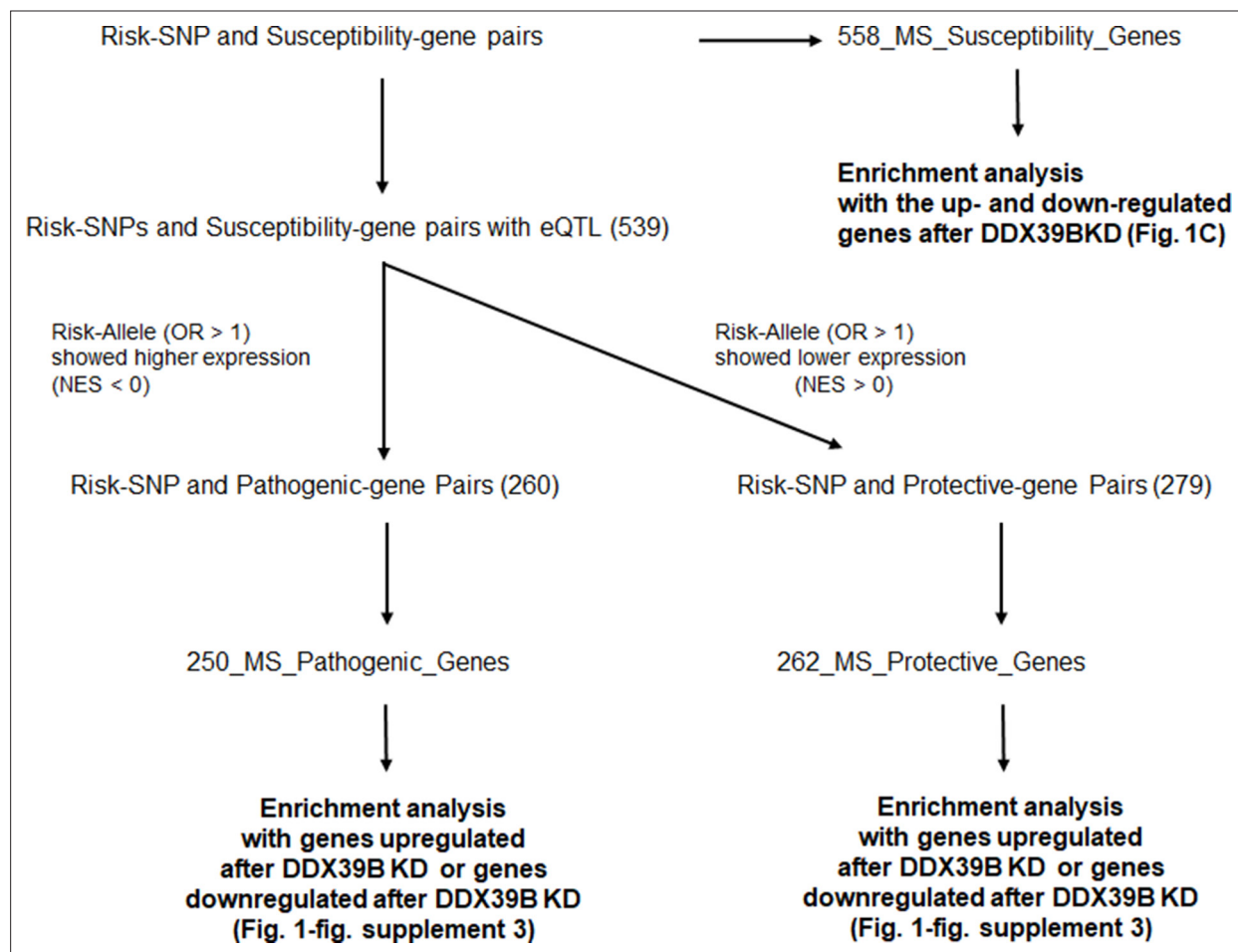


Figure 1—figure supplement 2. Schematic diagram of the enrichment analysis of MS-susceptibility genes among genes whose expression is altered by DDX39B knockdown. List of odds ratio (OR) of Risk-SNP and Susceptibility genes were obtained from *Patsopoulos et al., 2019*. Detail of the classification is described in the Methods section. The list of the MS_Pathogenic and MS_Protective genes is shown in *Supplementary file 3*.

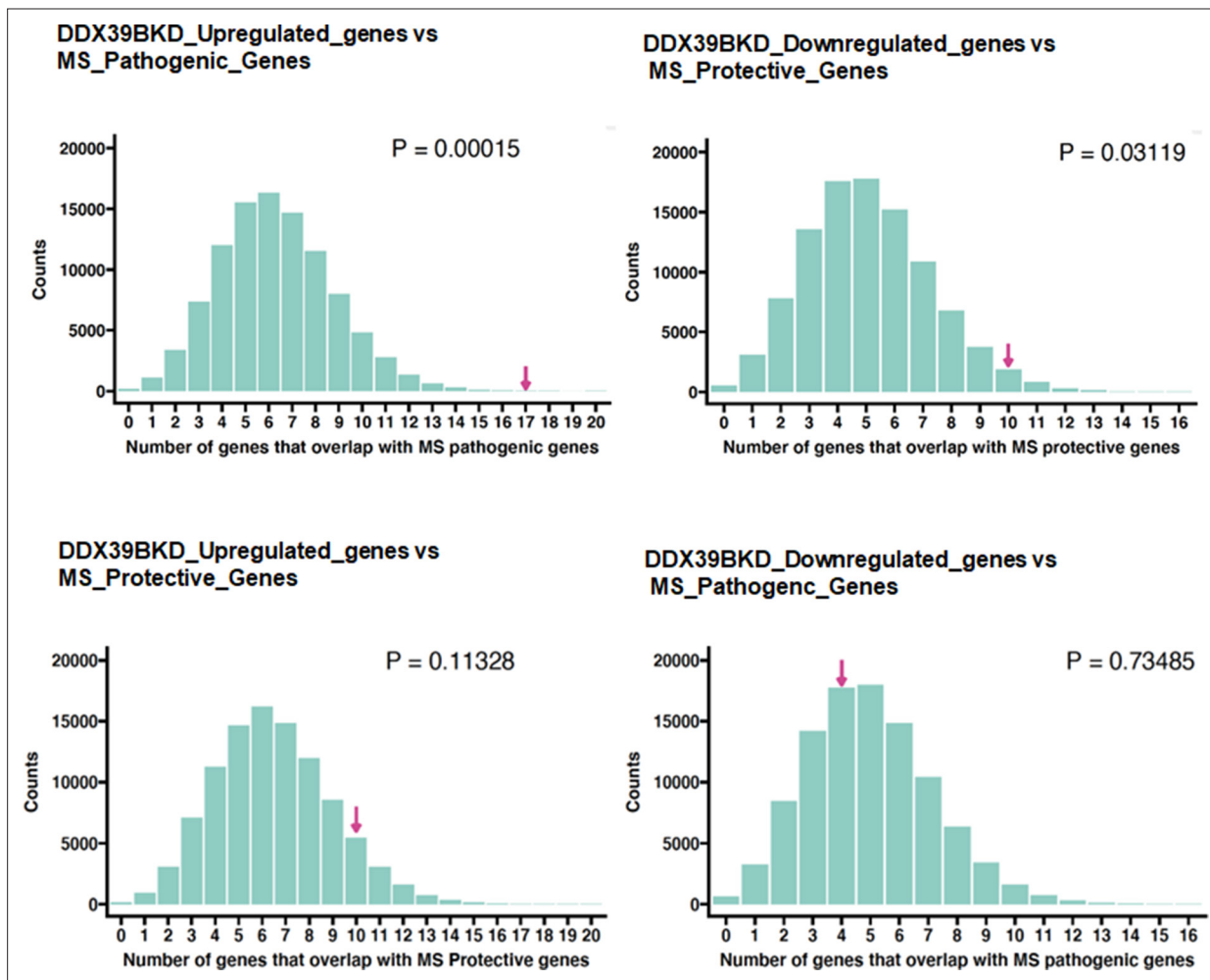


Figure 1—figure supplement 3. Enrichment analysis of the MS_Pathogenic or MS_Protective genes. Resampling 100,000 times resulted in a distribution of the number of genes that overlap by chance with experimental overlap indicated by magenta arrow. p Value was calculated based on the fraction of instances. Details of the analysis are described in the Materials and methods section.

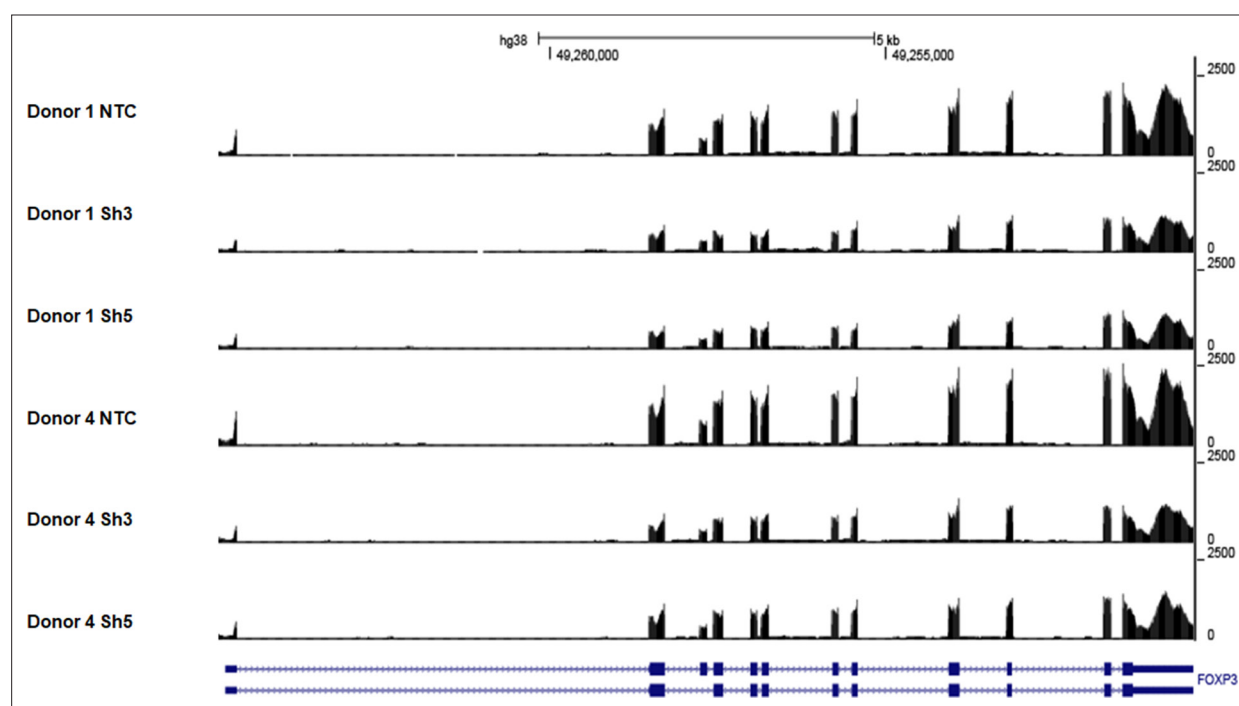


Figure 1—figure supplement 4. Coverage tracks of reads mapping to the *FOXP3* gene in control and DDX39B-depleted CD4⁺ T cells. The figure shows coverage of RNAseq reads mapping to the *FOXP3* gene in control (NTC) or DDX39B-depleted (Sh3 or Sh5) CD4⁺ T cells from two healthy donors (Donors 1 and 4).

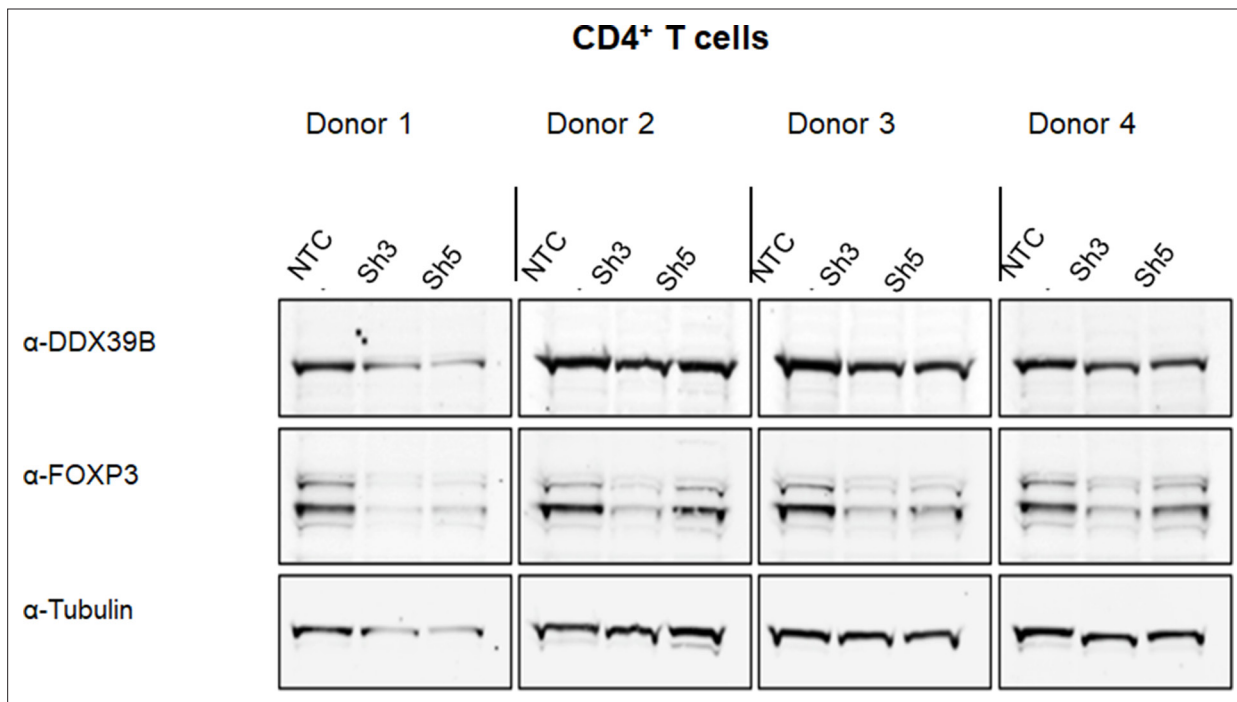


Figure 1—figure supplement 5. Western blot analysis of FOXP3 expression upon DDX39B depletion in CD4⁺ T cells. FOXP3 protein abundance was analyzed by western blot in CD4⁺ T cells from four donors transduced with either control (NTC) or DDX39B targeting (Sh3 or Sh5) shRNAs. The data were normalized to α -tubulin. Densitometry quantification of these data is shown in **Figure 1D**.

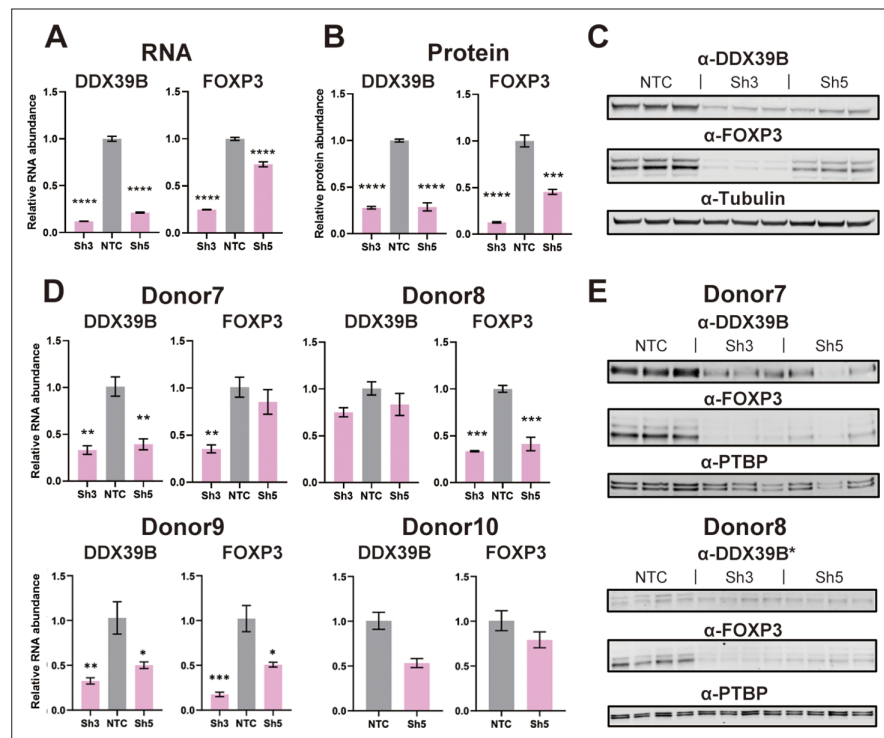


Figure 2. Effect of DDX39B depletion on FOXP3 RNA and protein expression. **(A)** Quantification of DDX39B and FOXP3 RNA between control (NTC) and DDX39B-depleted (Sh3 and Sh5) MT-2 cells. DDX39B and FOXP3 RNA abundance was measured by RT-qPCR and normalized to *EEF1A1* RNA expression. **(B)** Quantification of DDX39B and FOXP3 protein expression between control (NTC) and DDX39B-depleted (Sh3 and Sh5) MT-2 cells from western blot in **(C)**. DDX39B and FOXP3 protein abundance was normalized to α -tubulin. **(D)** DDX39B and FOXP3 expression upon DDX39B depletion in primary or induced Tregs. DDX39B was depleted in primary Tregs (Donors 7 and 8) and induced Tregs (Donors 9 and 10) via lentivirus transduction with either non-targeting control (NTC) or DDX39B targeting (Sh3 and/or Sh5) shRNAs. DDX39B and FOXP3 RNA abundance was measured by RT-qPCR and normalized to *EEF1A1* RNA expression. **(E)** Western blot of DDX39B and FOXP3 expression between control (NTC) and DDX39B-depleted (Sh3 and Sh5) primary Tregs. PTBP was used as a loading control. Error bars indicate SEM except for NTC in Donor 10 where error bars represent range due to loss of one replicate sample; *: $p < 0.05$, **: $p < 0.01$, ***: $p < 0.001$ and ****: $p < 0.0001$.

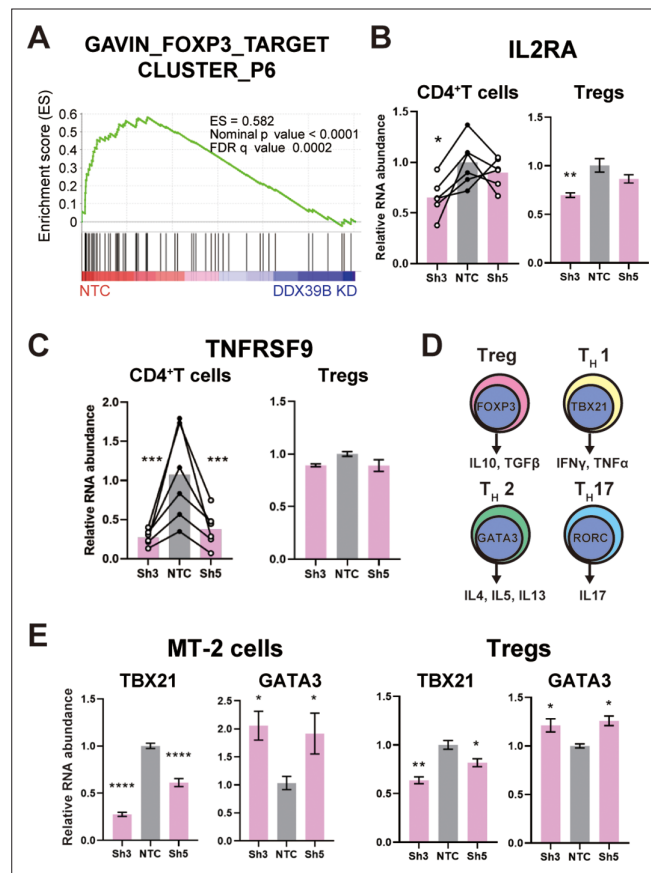


Figure 3. DDX39B depletion causes loss of Treg gene expression signature. **(A)** GSEA results of GAVIN_FOXP3_TARGET_CLUSTER_P6 gene set enriched in normal over DDX39B depleted CD4⁺ T cells **(B)** RNA abundance of IL2RA (CD25) relative to EE1A1 in DDX39B-depleted CD4⁺ T cells (Left) and primary Tregs (Right). **(C)** RNA abundance of TNFRSF9 relative to EE1A1 in DDX39B-depleted CD4⁺ T cells (Left) and primary Tregs (Right). **(D)** Schematic of genes expressed in different T cell lineages: Tregs, T_H1, T_H17, and T_H2 effector cells. **(E)** RNA abundance of transcription factors regulating T cell differentiation: TBX21 (T_H1), GATA3 (T_H2) in MT-2 cells (Left) and primary Tregs (Right). *: p<0.05, **: p<0.01, ***: p<0.001 and ****: p<0.0001.

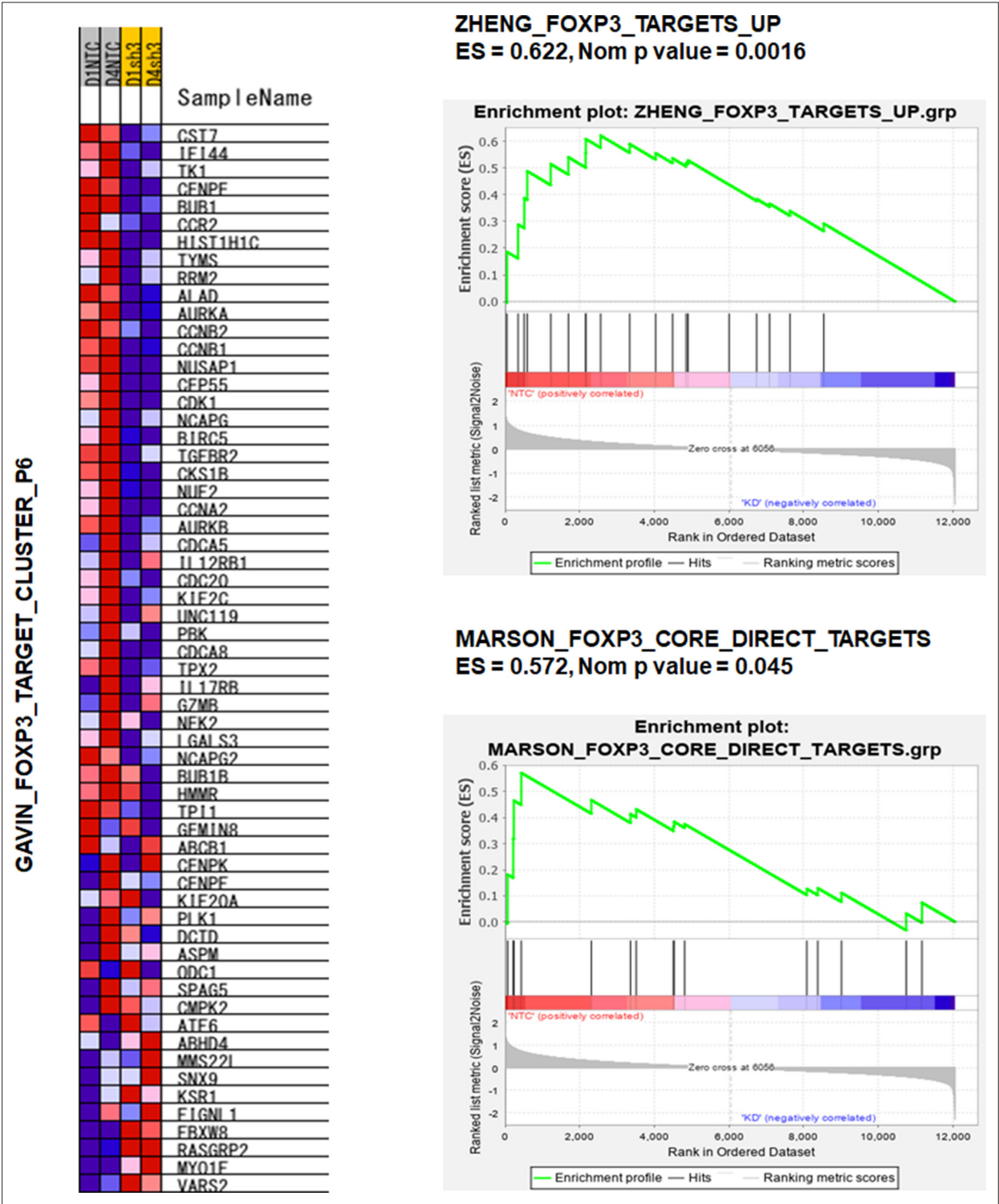


Figure 3—figure supplement 1. GSEA results of FOXP3-related gene sets enriched in normal over DDX39B-depleted cells. GSEA was conducted comparing the transcriptome of control (NTC) and DDX39B-depleted (Sh3) CD4⁺ T cells. Additional data for the GAVIN_FOXP3_TARGET_CLUSTER_P6 gene set are shown in *Figure 3A*.

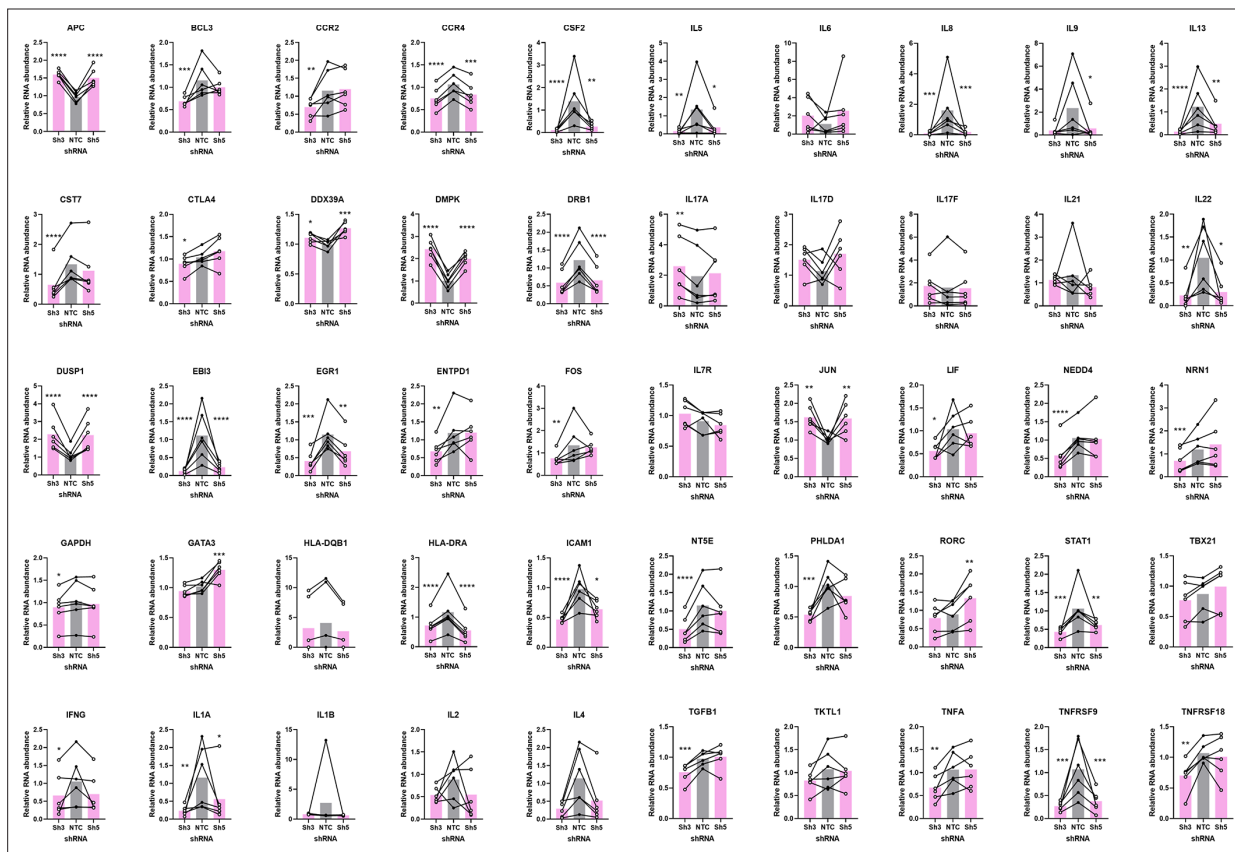
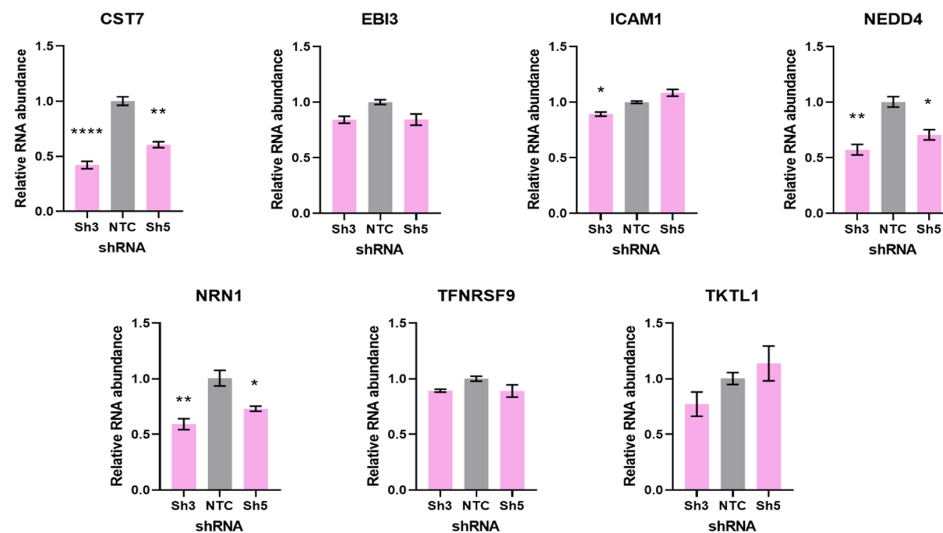


Figure 3—figure supplement 2. Effect of DDX39B depletion on expression of genes in CD4⁺ T cells. Expression of genes with known immune function and GAPDH (as a control), normalized to *EEF1A1* expression, was measured by RT-qPCR in control (NTC) or in primary CD4⁺ T cells depleted of DDX39B (Sh3 or Sh5) shRNAs. *: $p < 0.05$, **: $p < 0.01$, ***: $p < 0.001$ and ****: $p < 0.0001$.

Donor 7



Donor 8

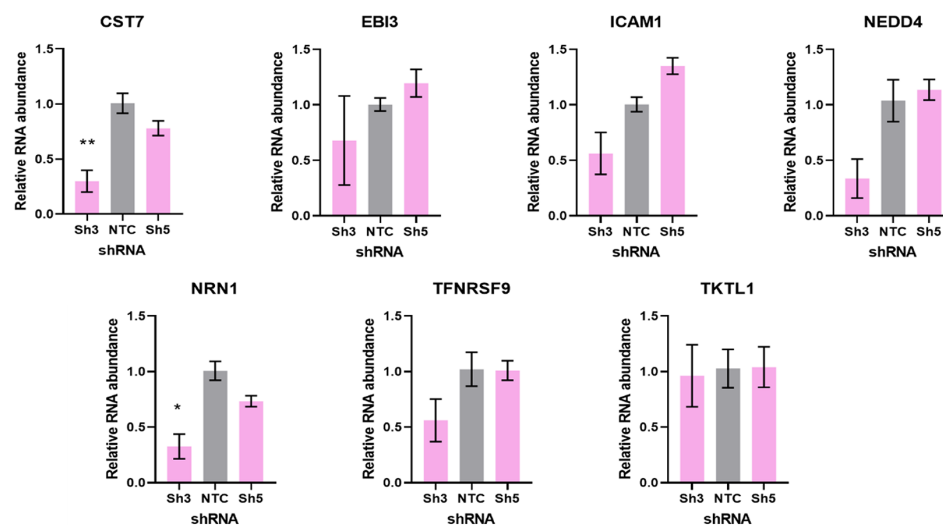


Figure 3—figure supplement 3. Effect of DDX39B depletion on expression of Treg genes. DDX39B was depleted in T regs from Donors 7 and 8, and expression of seven Treg-related genes (from Gavin et al., 2007) were measured by RT-qPCR and normalized to *EEF1A1* expression. *: $p < 0.05$, **: $p < 0.01$ and ****: $p < 0.0001$.

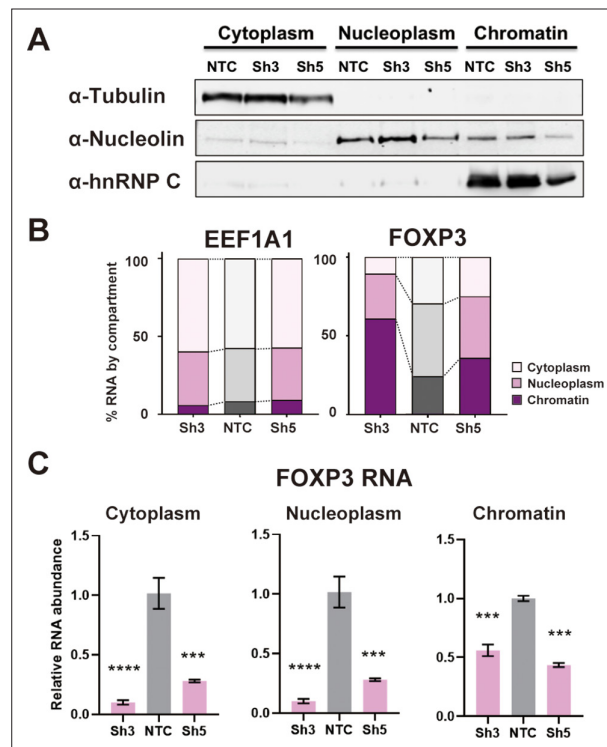


Figure 4. DDX39B depletion disturbs an early step in FOXP3 RNA biogenesis. **(A)** Protein abundance of subcellular compartment markers in fractionated control (NTC) or DDX39B-depleted (Sh3 and Sh5) MT-2 cells. **(B)** Percent EE1A1 or FOXP3 RNA in subcellular compartments. **(C)** FOXP3 RNA abundance relative to EE1A1 in subcellular compartments upon DDX39B depletion.

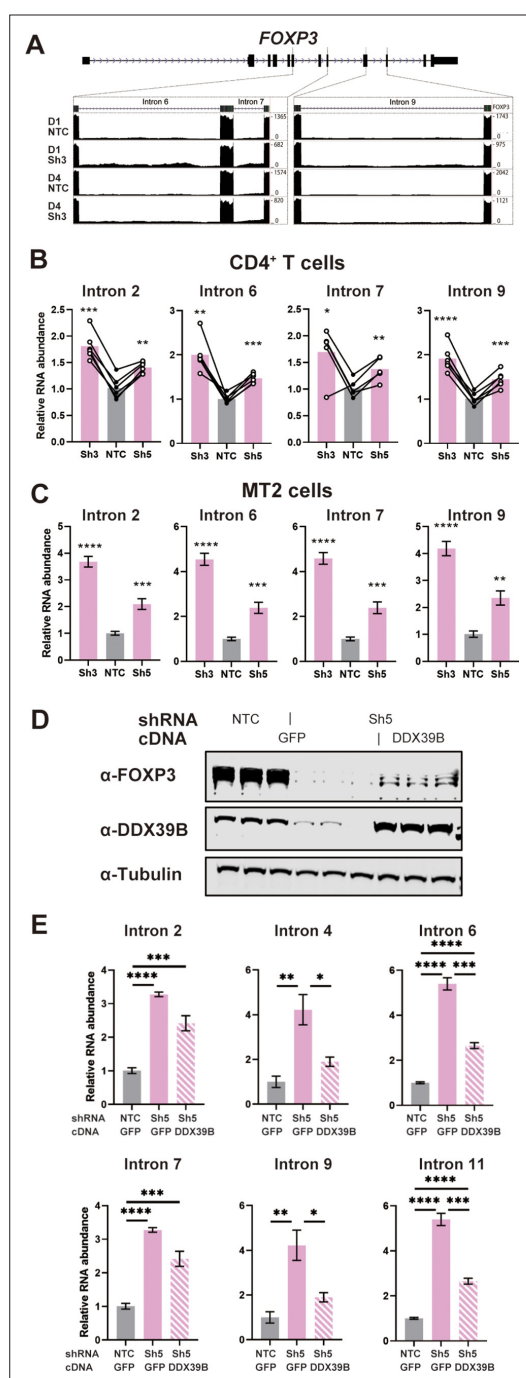


Figure 5. DDX39B depletion triggers the retention of FOXP3 introns. **(A)** RNAseq reads mapping to the FOXP3 genomic region in control (NTC) or DDX39B depleted (Sh3) CD4⁺ T cells from Donors 1 and 4. Read counts for FOXP3 introns 6, 7, and 9 are shown on the Y-axis in the two insets. **(B, C)** Abundance of FOXP3 RNA introns relative to total FOXP3 RNA after DDX39B depletion in CD4⁺ T cells from six donors **(B)** or MT-2 cells **(C)**. **(D–E)** Rescue of the DDX39B depletion (Sh3) by exogenous expression (GFP or DDX39B) in MT-2 cells. The abundance of FOXP3 and DDX39B relative to Tubulin **(D)** or FOXP3 RNA introns relative to total

Figure 5 continued on next page

Figure 5 continued

FOXP3 RNA (E) are shown. *: $p < 0.05$, **: $p < 0.01$, ***: $p < 0.001$ and ****: $p < 0.0001$.

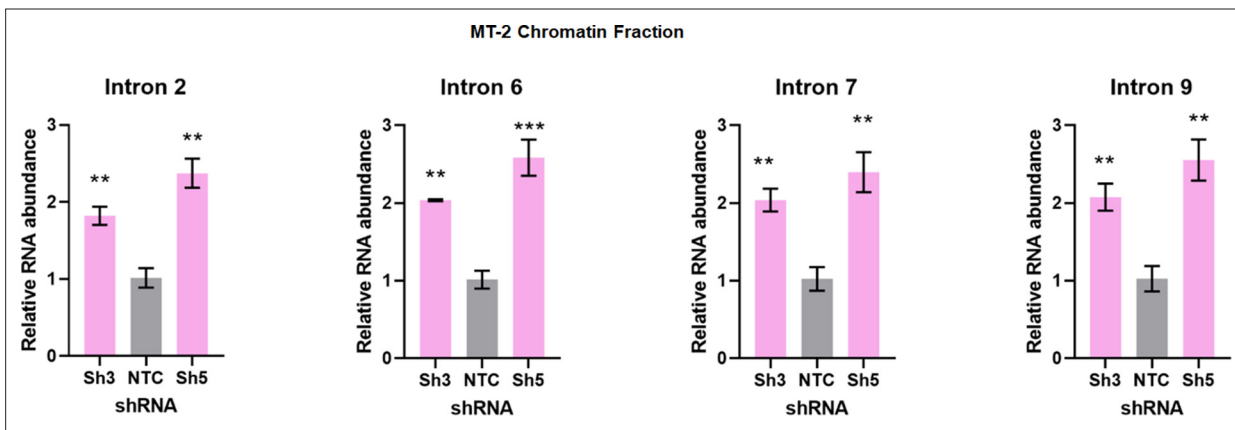
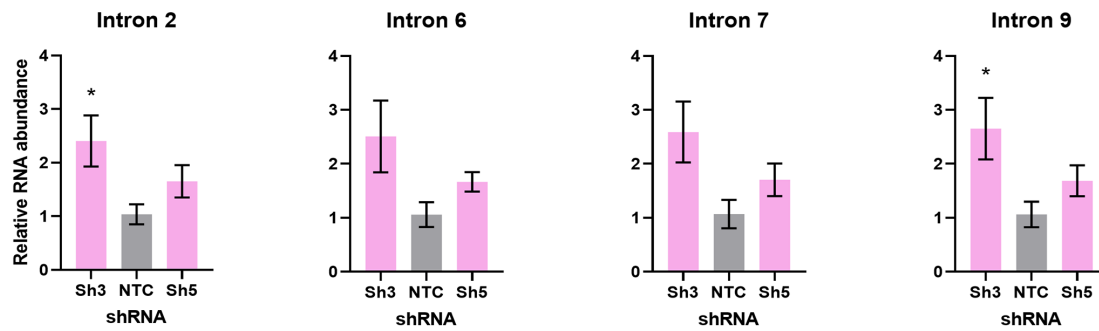
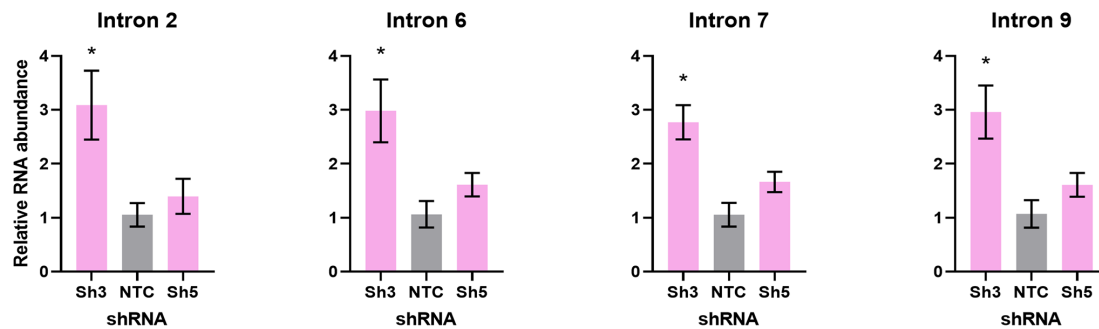


Figure 5—figure supplement 1. Quantification of *FOXP3* retained introns in the chromatin fraction of MT-2 cells. Control (NTC) or DDX39B-depleted (Sh3 or Sh5) MT-2 cells were fractionated into cytoplasm, nucleoplasm and chromatin fractions. Retained *FOXP3* introns were quantified in the chromatin compartment by RT-qPCR using intron-specific primers and normalized to total *FOXP3* RNA. **: $p < 0.01$, ***: $p < 0.001$.

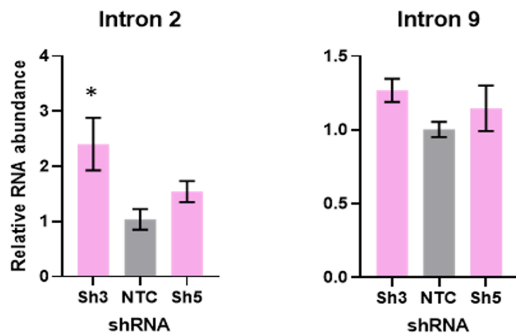
Donor 7



Donor 8



Donor 9



Donor 10

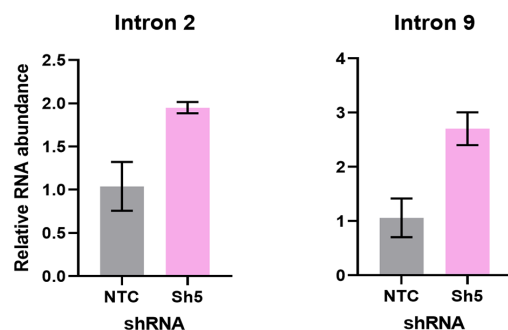


Figure 5—figure supplement 2. Quantification of *FOXP3* retained introns in primary and induced Tregs. DDX39B was depleted in Tregs from four independent donors (Donors 7–10) via lentivirus transduction with either control (NTC) or DDX39B targeting (Sh3 or Sh5) shRNAs. Retained *FOXP3* introns were quantified from total RNA by RT-qPCR using intron-specific primers and normalized to total *FOXP3* RNA. *: $p < 0.05$.

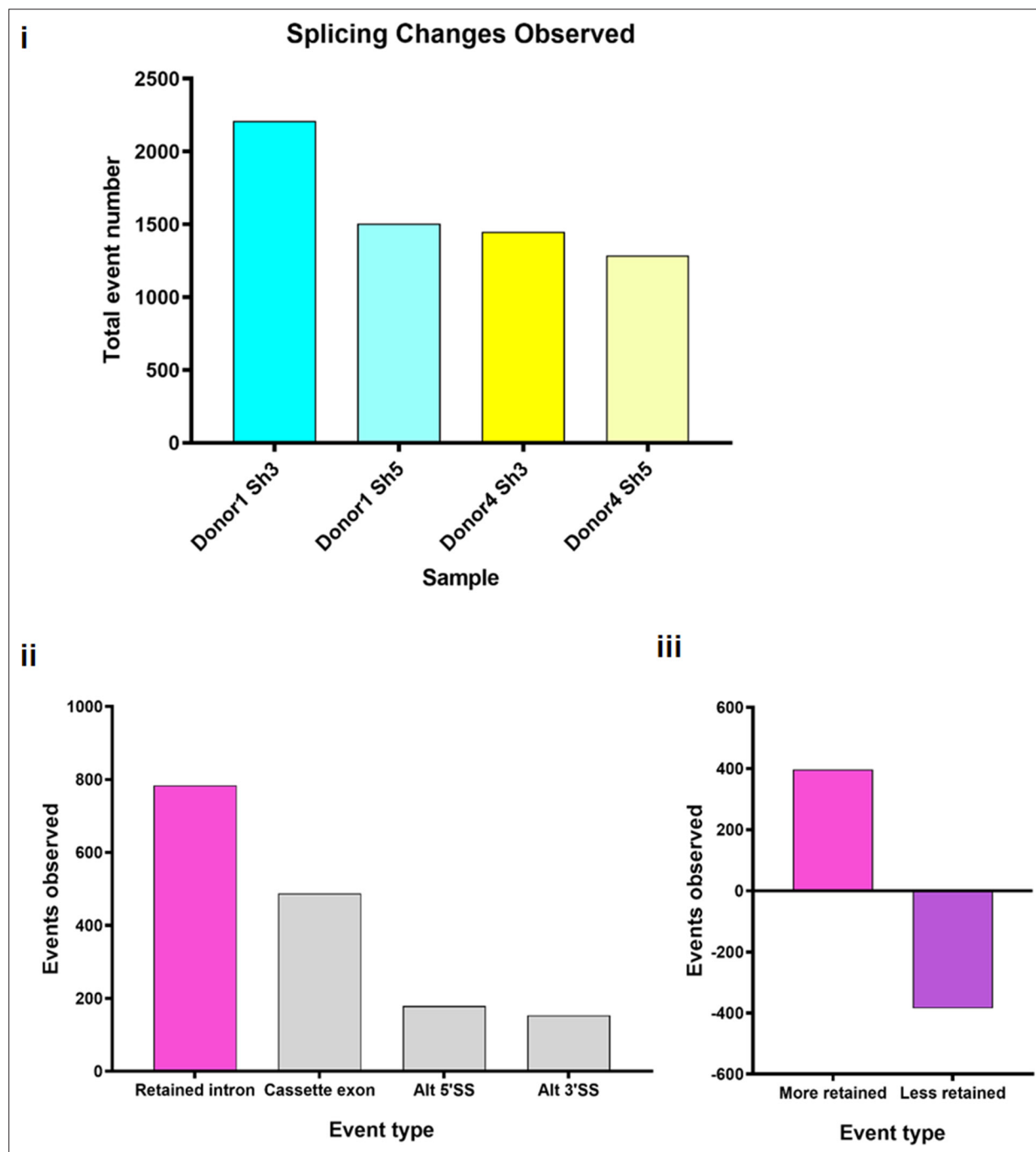


Figure 5—figure supplement 3. Alternative splicing events observed upon DDX39B depletion in CD4⁺ T cells. Splicing analysis of RNAseq data was carried out using Vast-Tools. (i) Total events changed between control and either of two knockdown conditions (Sh3 and Sh5) in two donors (donors 1 and 4). (ii) Type of events of Sh3 knockdown in either donor are shown. Alt 5'SS, alternative 5' splice site; Alt 3'SS, alternative 3' splice site. (iii) Intron retention events in either donor are divided into those showing more retention or less retention with DDX39B knockdown.

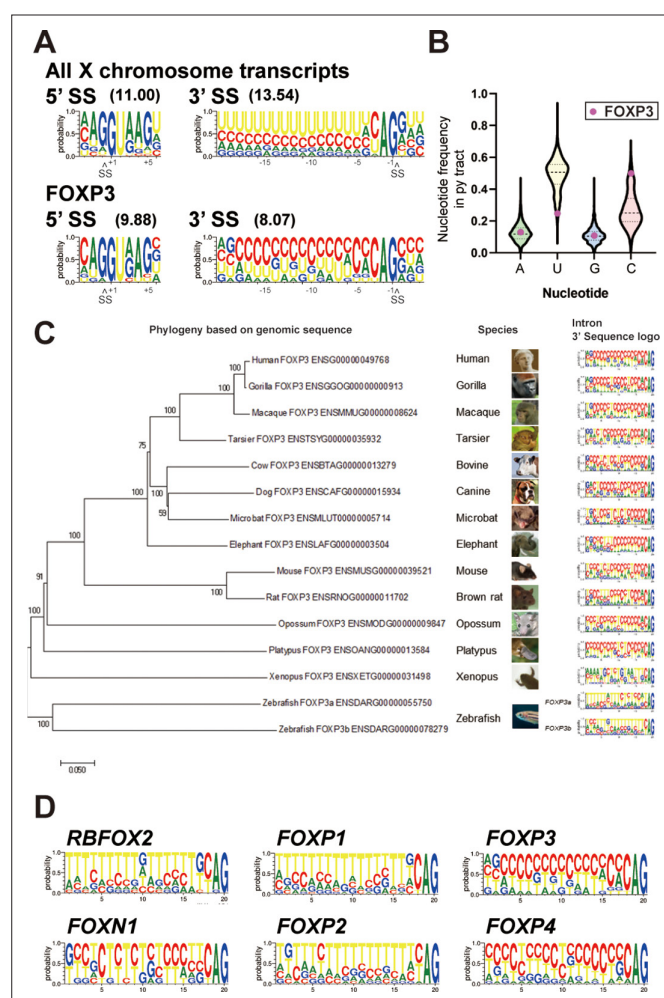


Figure 6. *FOXP3* introns have conserved C-rich py tracts. **(A)** Sequence logos of the 5' and 3' splice sites (SS) of *FOXP3* versus all other chromosome X genes. 5' or 3' MaxEntScore based on the highest-probability sequence are shown. **(B)** Distribution of the py tract nucleotide frequency among chromosome X genes. Magenta dots indicate *FOXP3*. **(C)** Phylogenetic tree and 3' SS sequence logos of the *FOXP3* among 14 species. Zebrafish has two *FOXP3* genes (*FOXP3a* and *FOXP3b*). **(D)** 3' SS sequence logos of *FOX* family genes. *RBFOX2* is shown as an outgroup.

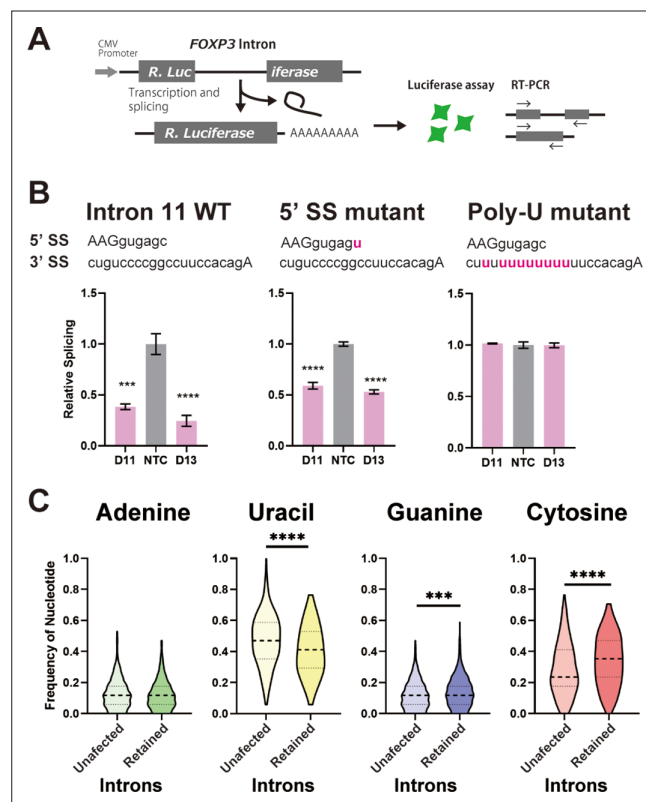


Figure 7. C-rich py tracts in *FOXP3* introns determine DDX39B sensitivity. **(A)** Schematic diagram of the splicing reporter. **(B)** Relative splicing efficiency of the wild-type (WT) or mutant (5' SS mutant and Poly-U mutant) *FOXP3* intron 11 splicing reporters after DDX39B depletion with D11 and D13 siRNAs. The sequence of 5' splice sites (5' SS) for these introns is shown indicating the three upstream exonic residues in capital letters and the six downstream intronic residues in minuscule letters. The sequence of the py tracts and 3' splice sites (3' SS) for these introns is shown indicating the intronic residues in minuscule letters and a single exonic residue in capital letters. **(C)** Nucleotide frequency in the py tract of introns that are insensitive (unaffected) or sensitive (retained) to DDX39B depletion. *: $p < 0.05$, **: $p < 0.01$, ***: $p < 0.001$ and ****: $p < 0.0001$.

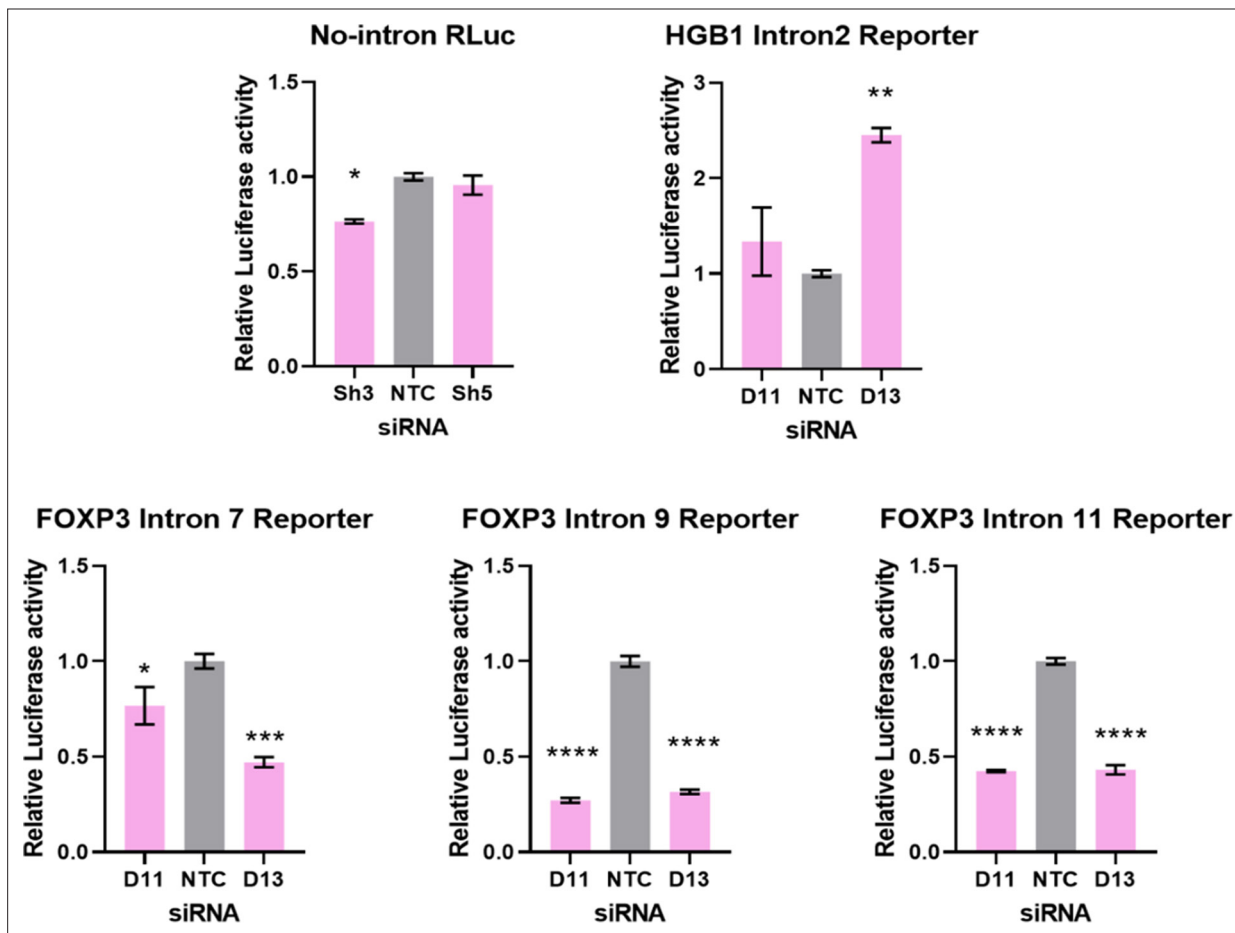


Figure 7—figure supplement 1. Luciferase activity of the splicing reporters. Control (NTC) or DDX39B-depleted (D11 or D13 siRNAs) HeLa cells were co-transfected with a Firefly luciferase reporter (transfection control, FLuc) and Renilla luciferase (RLuc) splicing reporters with no intron, human β globin (HGB1) intron 2, or FOXP3 introns 7, 9, or 11. Relative splicing efficiency of reporters was inferred by measuring luciferase activity (RLuc/FLuc) normalized to NTC. *: $p < 0.05$, **: $p < 0.01$, ***: $p < 0.001$ and ****: $p < 0.0001$.

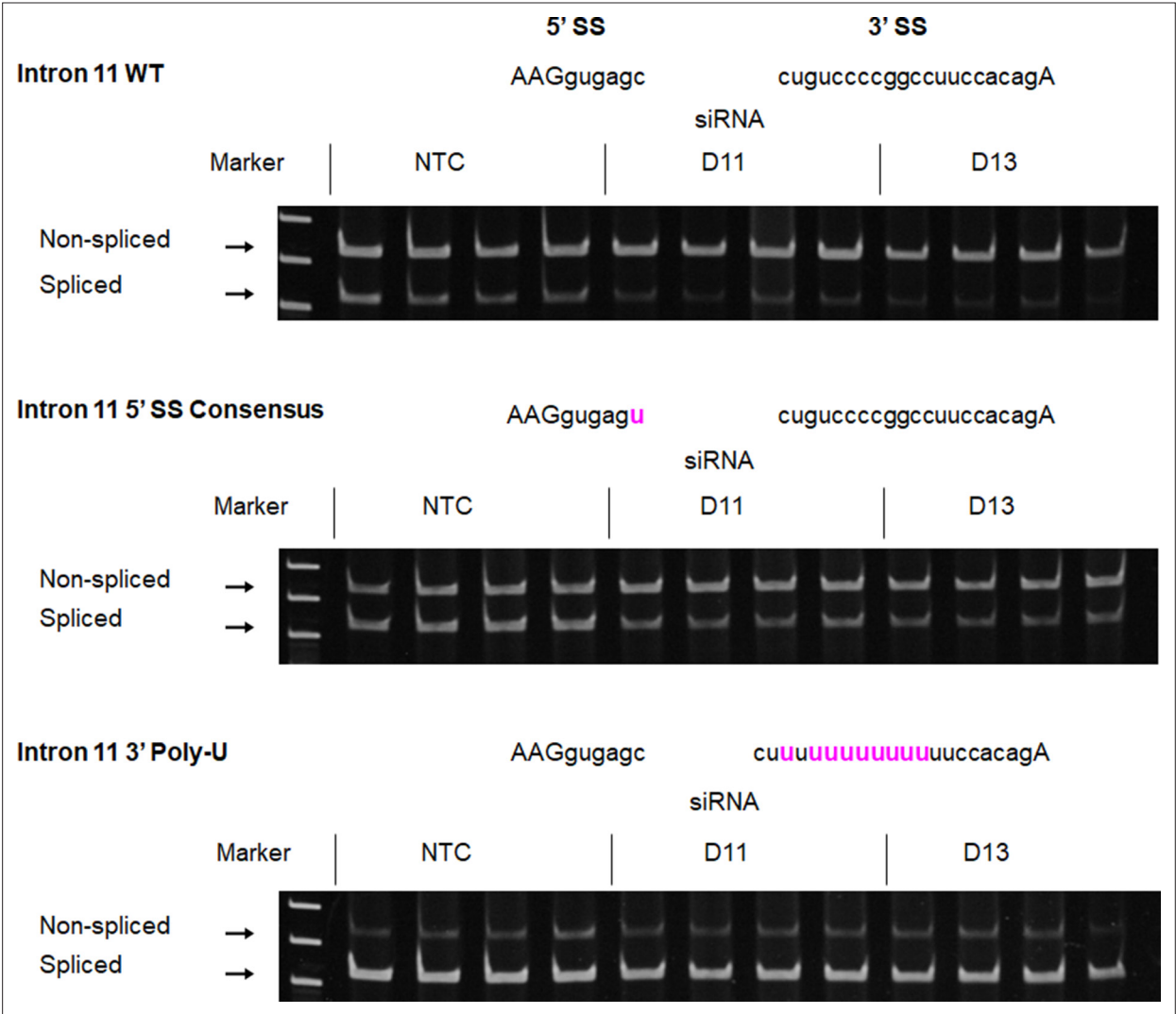


Figure 7—figure supplement 2. RT-PCR analysis of splicing efficiency of wild-type or mutant *FOXP3* Intron 11 RLuc reporters. Control (NTC) or DDX39B-depleted (D11 or D13) HeLa cells were transfected with *FOXP3* intron 11 RLuc reporters (WT, 5' SS consensus or 3' Poly-U mutant), and splicing efficiency was directly measured by endpoint RT-PCR. Quantification of the gels is shown in **Figure 7B**.

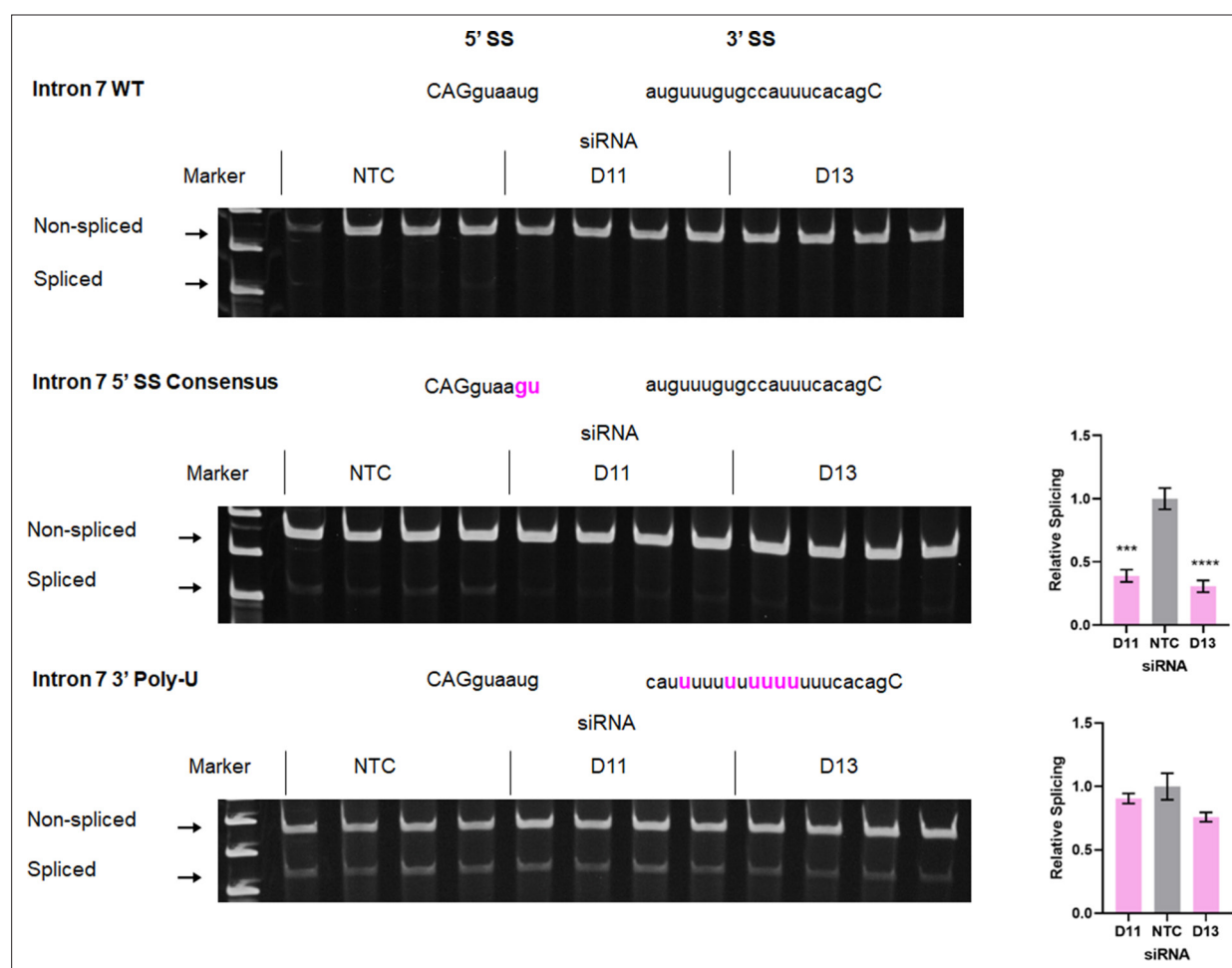


Figure 7—figure supplement 3. RT-PCR analysis of splicing efficiency of wild-type or mutant *FOXP3* Intron 7 RLuc reporters. Control (NTC) or DDX39B-depleted (D11 or D13) HeLa cells were transfected with *FOXP3* intron 7 RLuc reporters (WT, 5' SS consensus or 3' Poly-U mutant), and splicing efficiency was directly measured by endpoint RT-PCR. Quantification is shown on the right for the lower two panels; given the very low level of splicing with intron 7 WT reporter it could not be accurately quantified. ***: $p < 0.001$ and ****: $p < 0.0001$.

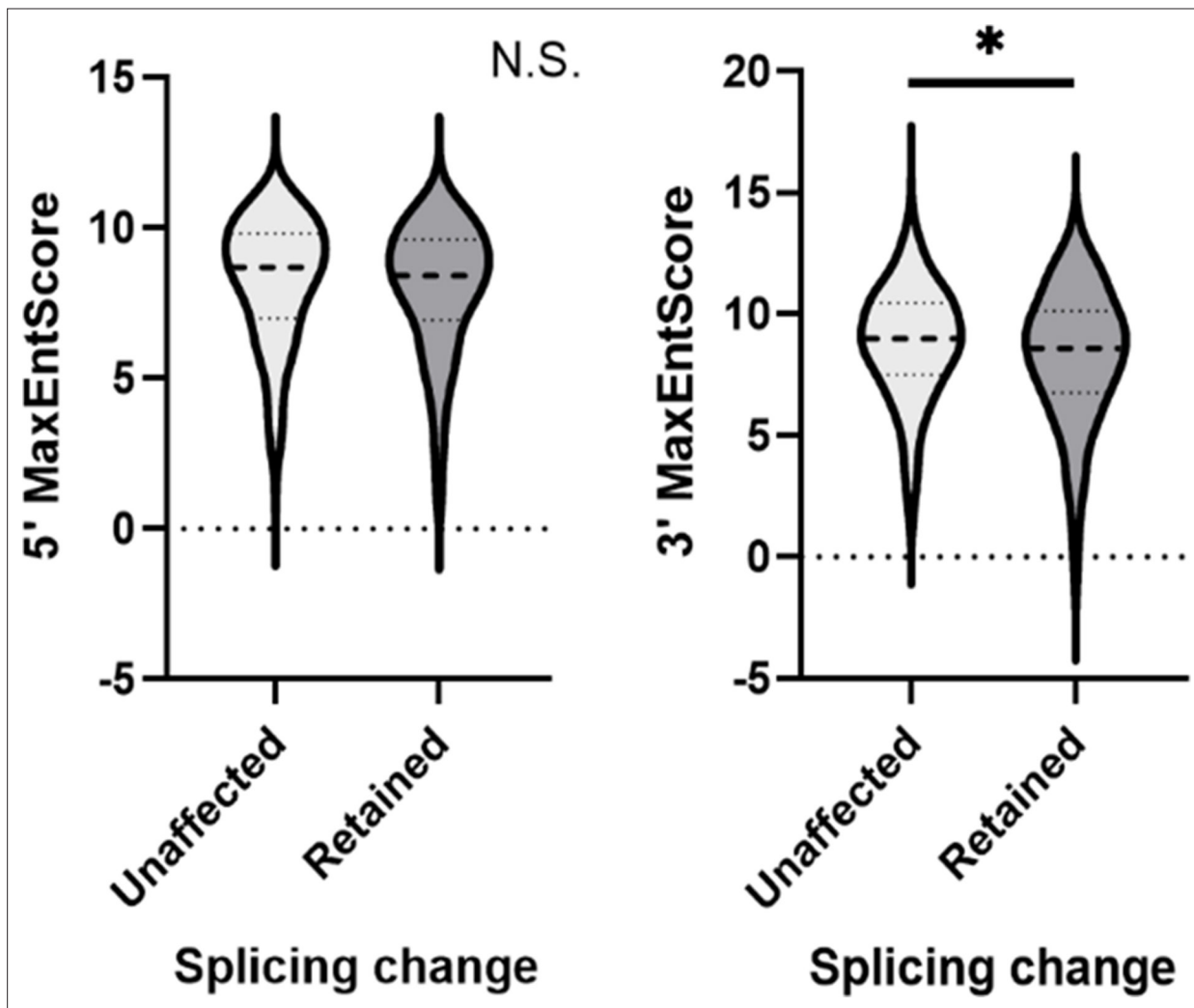


Figure 7—figure supplement 4. Comparison of Max entropy splice sites (SS) score between unaffected and DDX39B-sensitive introns. Max entropy score of 5' SS and 3' SS of unaffected (500 randomly selected) and introns with increased retention upon DDX39B depletion (397 events) was determined using *MaxEntScan* (Yeo G and Burge CB, 2004). Dashed lines within the violin plots denote median values. *: $p < 0.05$.

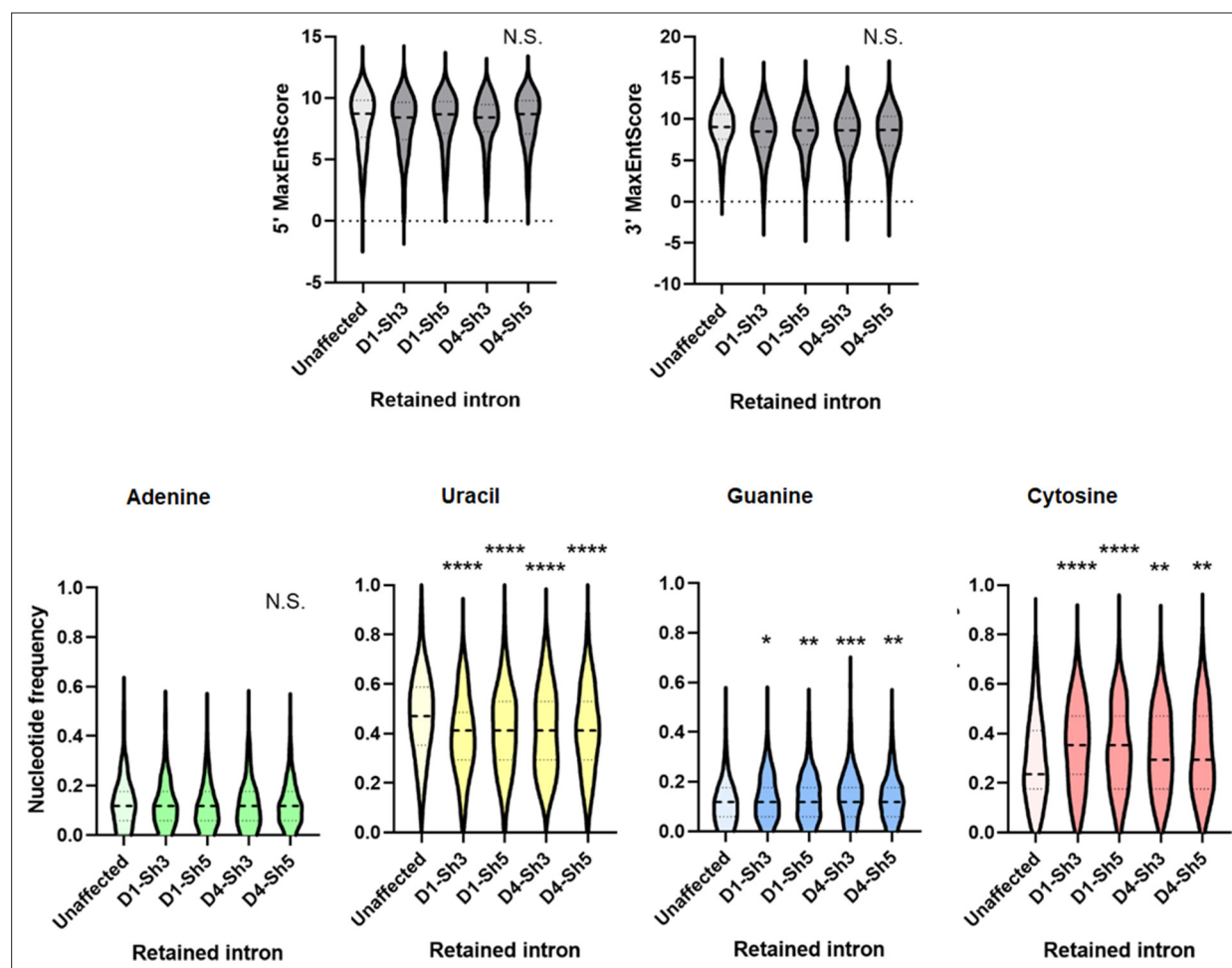
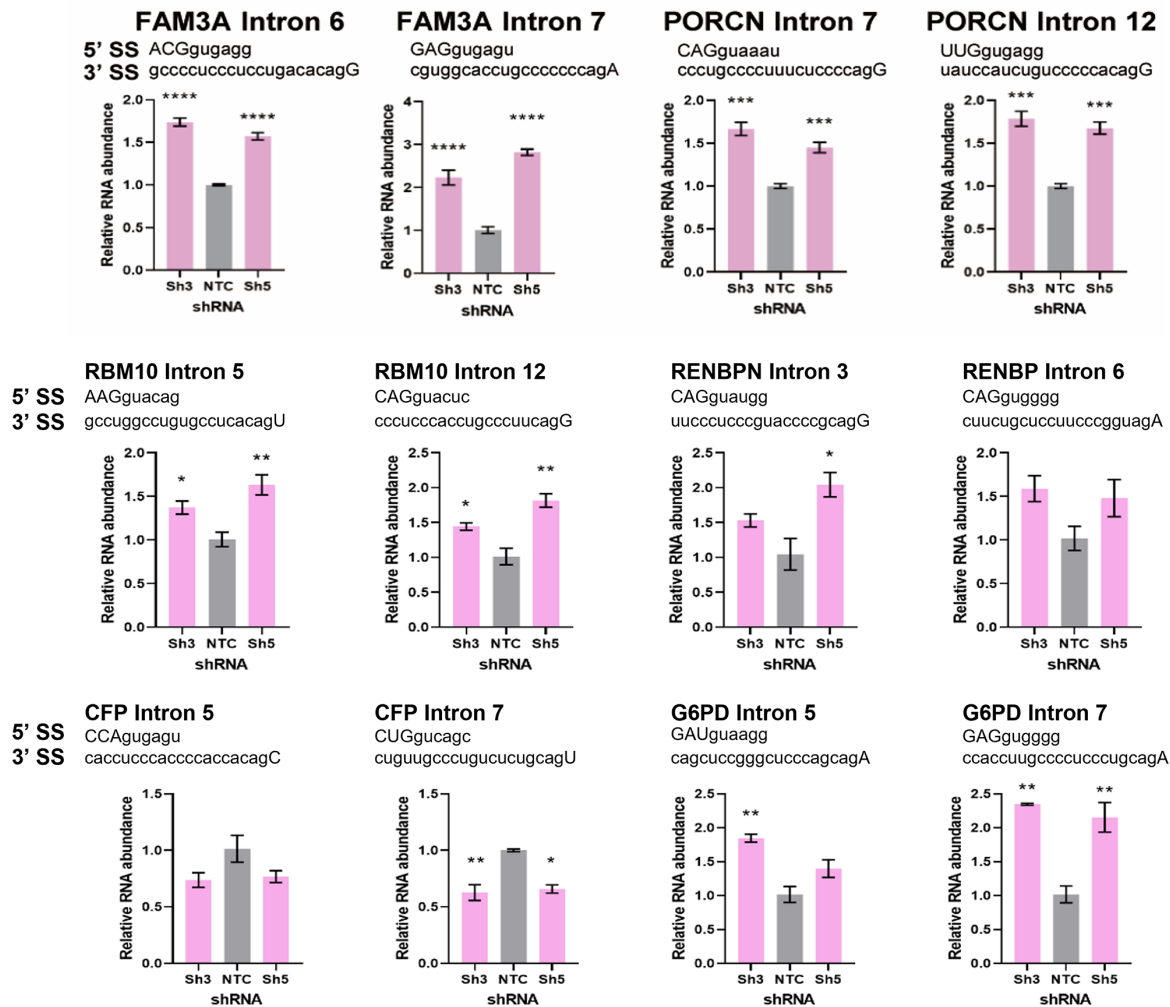


Figure 7—figure supplement 5. Comparison of Max entropy splice site (SS) scores (top panel) and nucleotide composition of py tracts (bottom panel) of unaffected introns or introns that were more retained in CD4⁺ T cells from either donor 1 or 4 depleted of DDX39B by treatment with Sh3 or Sh5. *: $p < 0.05$, **: $p < 0.01$, ***: $p < 0.001$ and ****: $p < 0.0001$.

C-rich py tract genes



U-rich py tract genes

Figure 7—figure supplement 6. Detection of intron retention events in X chromosome genes with C-rich or U-rich py tracts. Introns of the transcripts with C-rich (top) or U-rich (bottom) py tract were quantified by intron-specific RT-qPCR in control (NTC) and DDX39B-depleted (Sh3 or Sh5) MT-2 cells and normalized to their corresponding total transcripts. *: $p < 0.05$, **: $p < 0.01$, ***: $p < 0.001$ and ****: $p < 0.0001$.

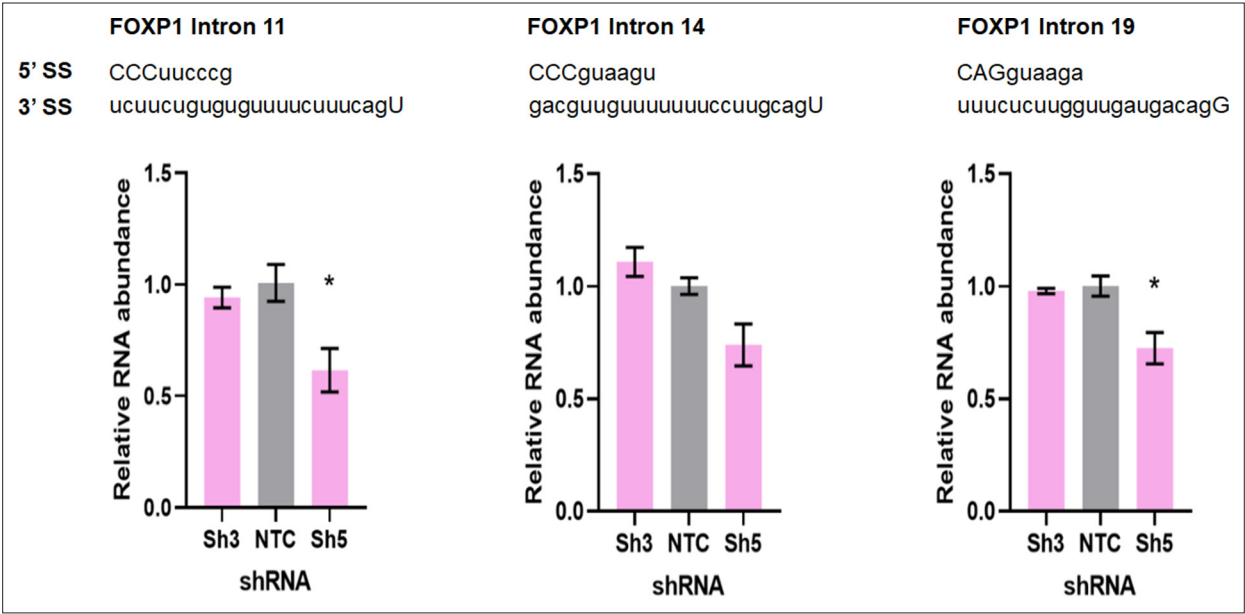


Figure 7—figure supplement 7. Retention of *FOXP1* introns is not increased upon DDX39B depletion in MT-2 cells. *FOXP1* transcripts including introns 11, 14, or 19 were quantified by intron-specific RT-qPCR in control (NTC) and DDX39B-depleted (Sh3 or Sh5) MT-2 cells and normalized to total *FOXP1* transcripts. *: p<0.05.

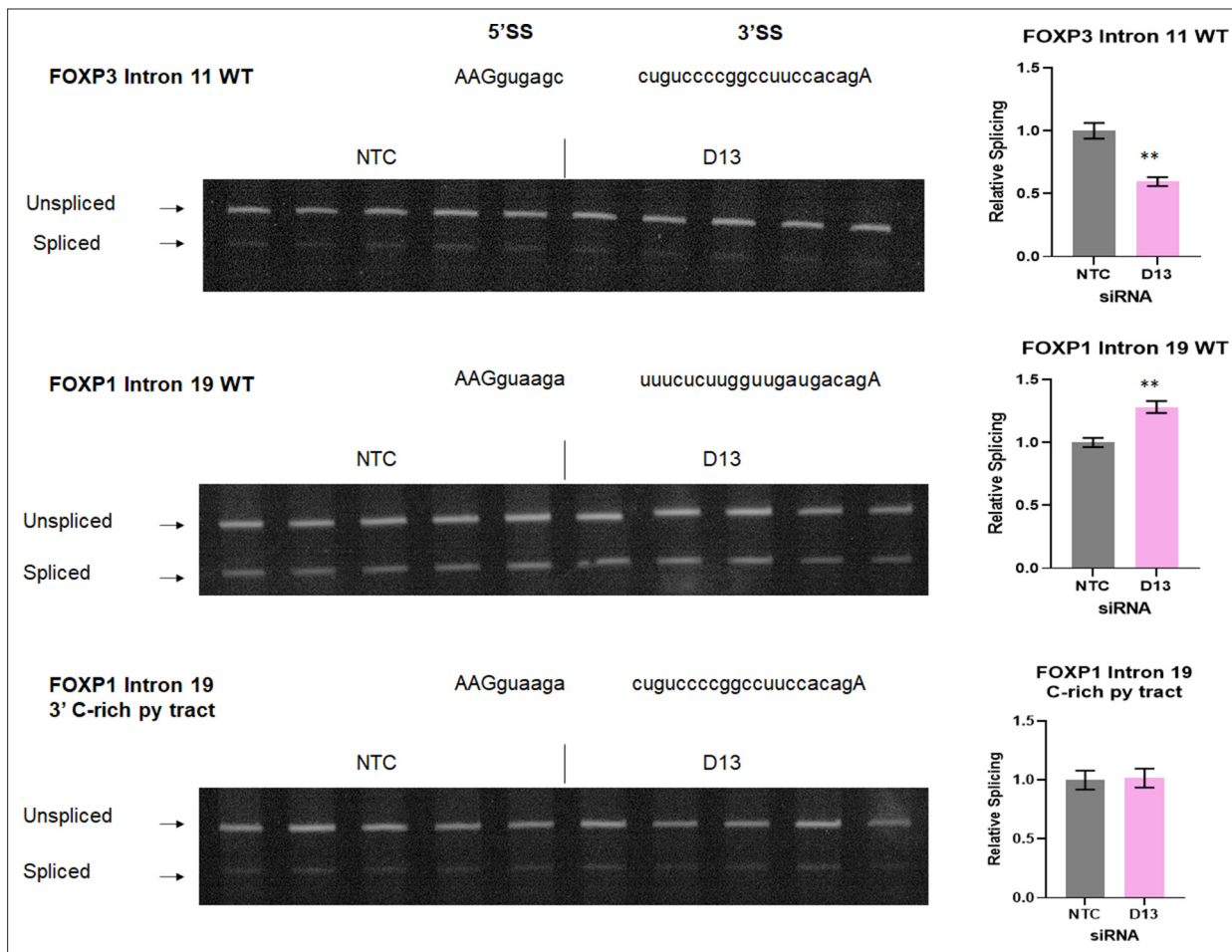


Figure 7—figure supplement 8. RT-PCR analysis of splicing efficiency of wild-type or mutant *FOXP1* Intron 19 RLuc reporters. Control (NTC) or DDX39B-depleted (D13) HeLa cells were transfected with *FOXP3* or *FOXP1* RLuc reporters. Splicing efficiency was directly measured by endpoint RT-PCR. Quantification is shown on the right. **: $p < 0.01$.

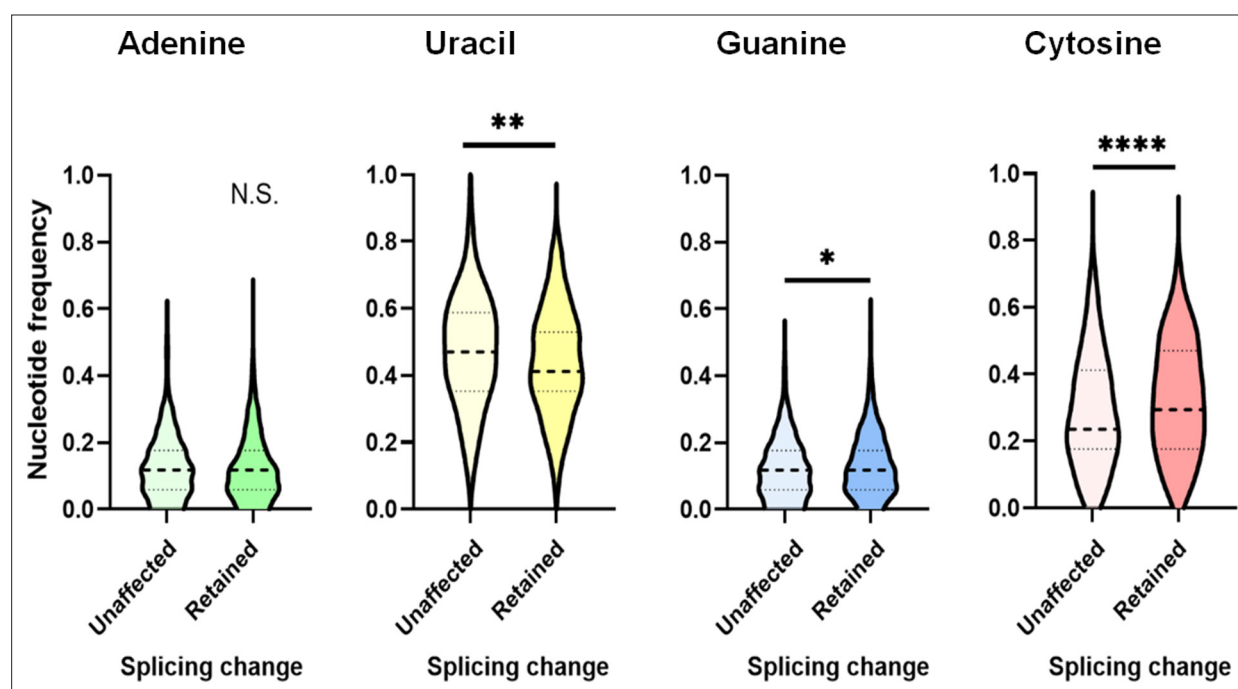


Figure 7—figure supplement 9. Comparison of py tract composition between unaffected and less-retained introns. Nucleotide frequency of py tracts of unaffected (500 randomly selected) and those that are less-retained upon DDX39B knockdown (387) was calculated. Dashed lines denote median values. $p < 0.05$, *: $p < 0.01$, **: $p < 0.001$ and ****: $p < 0.0001$.

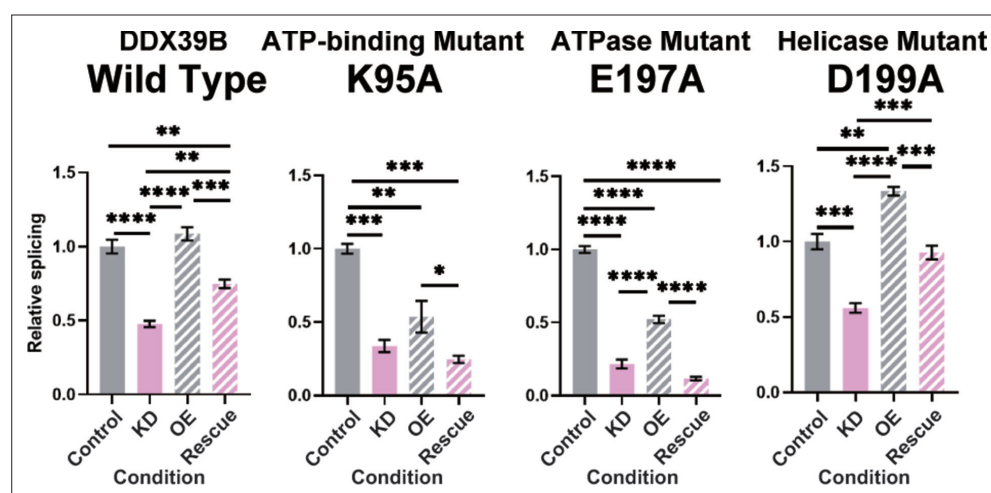


Figure 8. *FOXP3* intron 11 splicing requires DDX39B ATPase activity but not its helicase activity. Rescue of the splicing of *FOXP3* intron 11 reporter by induced expression of wild type (WT) or mutant (K95A, E197A, and D199A) DDX39B. KD and OE indicate knockdown and over-expression, respectively. *: $p < 0.05$, **: $p < 0.01$, ***: $p < 0.001$ and ****: $p < 0.0001$.

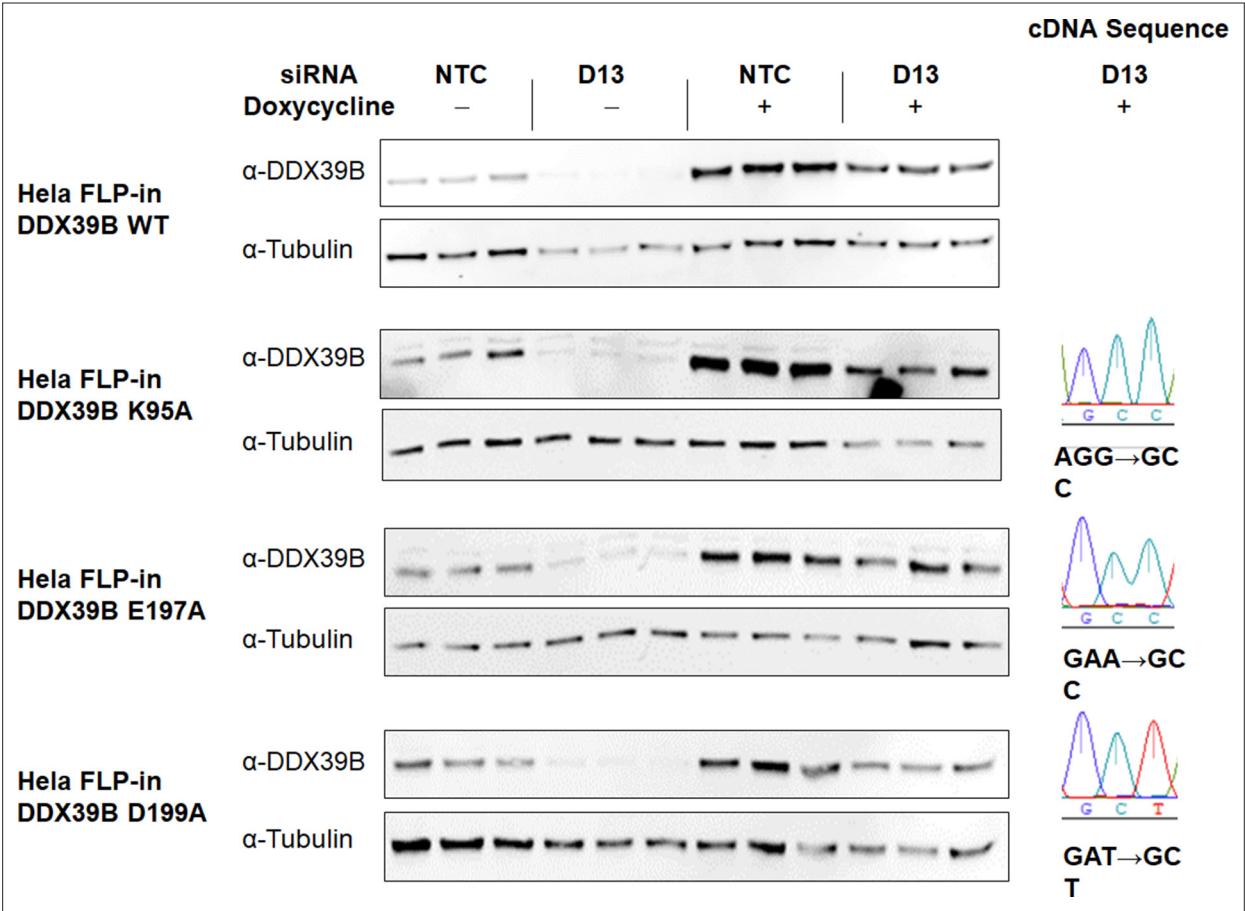


Figure 8—figure supplement 1. Expression of WT or mutant DDX39B in stable cell lines. Stable HeLa cell lines with inducible expression of WT or mutant DDX39B *trans*-genes were transfected with control (NTC) or DDX39B (D13) siRNAs, and expression of a siRNA-resistant DDX39B transgene was induced with Doxycycline. DDX39B protein expression was quantified by western blot (left). Sanger sequencing of DDX39B RT-PCR amplicons from rescue with mutant DDX39B *trans*-genes (D13 +Doxycycline) shows preferential expression of DDX39B *trans*-genes under rescue conditions (right).